ACS Macro Letters

pubs.acs.org/macroletters Letter

Exo-selective, Reductive Heck Derived Polynorbornenes with Enhanced Molecular Weights, Yields, and Hydrocarbon Gas Transport Properties

Benjamin J. Sundell,*,‡ John A. Lawrence, III,*,‡ Daniel J. Harrigan, Sibo Lin, Tatiana P. Headrick, Jeremy T. O'Brien, William F. Penniman, and Nathan Sandler

Cite This: *ACS Macro Lett.* 2020, 9, 1363−1368 Read Online

ACCESS | Metrics & More | Article Recommendations | Supporting Information

ABSTRACT: Next-generation membranes use highly engineered polymeric structures with enhanced chain rigidity, yet difficulties in polymerization often limit molecular weights required for film formation. Addition-type polynorbornenes are promising materials for industrial gas separations, but suffer from these limitations owing to *endo*−*exo* monomeric mixtures that restrict polymerization sites. In this work, a synthetic approach employing the reductive Mizoroki−Heck reaction resulted in *exo*-selective products that polymerized up to >99% yields for ROMP and addition-type polymers, achieving molecular weights an order of magnitude higher than addition-type polymers from *endo*−*exo* mixtures and impressive side group stereoregularity. Due to this increased macromolecular control, these polynorbornenes demonstrate unique solubility-selective permeation with mixed gas selectivities that exceed commercially used PDMS. In addition to thermal and structural characterization, XRD and computational studies confirmed the results of pure and mixed-gas transport testing, which show highly rigid membranes with favorably disrupted chain packing.

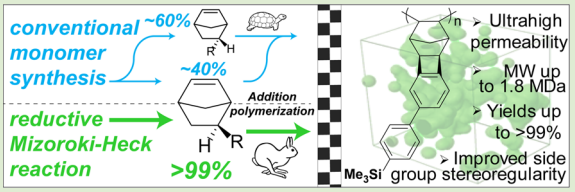

Membrane technology has profoundly impacted our world by offering solutions to global water shortages via reverse osmosis desalination, medical improvements for dialysis, and increased energy efficiency in gas purification compared to distillation- and absorption-based technologies.[1−3] With regard to gas separations, membranes are well positioned to alleviate both environmental challenges in CO_2 sequestration and industrial problems in natural gas upgrading.[4−6] Gas separation membranes typically operate by preferentially permeating smaller gases compared to larger gases, which becomes difficult when light hydrocarbon gases contain similar kinetic diameters and polarities to methane. Challenges further arise in the industrially important separation of natural gas liquids (NGL, e.g., propane and butane) from methane when using standard, size-discriminating membranes because high recompression costs of a CH_4-rich permeate limit economic viability. Instead, processing plants utilize a reverse-selective paradigm that permeates larger gases preferentially by exploiting the favorable sorption of relatively condensable penetrants.[7−10]

The NGL separation makes up a significant portion of the $100 million/year vapor recovery membrane market,[5] and recently developed, highly rigid and porous glassy polymers show promise in displacing commercial rubbery materials. Despite their combinations of high gas selectivity (C_{3+}/CH_4) and C_{3+} gas permeability, highly glassy polymers may face difficulties in polymerization to large molecular weight at efficient yields,[11,12] often exacerbated by stereochemical differences in the starting materials.[13]

Our previous work in polymerizing addition-type polynorbornenes showed that the presence of *endo*-isomeric monomers reduced polymer yields[14] and even precluded polymerizations in subsequent studies. The work of Yampolskii et al., Tetsuka et al., Rhodes et al., and Long et al. also observed these difficulties.[12,15−17] Separately, pioneering work in the Register group developed living addition-type polynorbornenes and block copolymers that demonstrated greatly reduced reactivity ratios in *endo*-isomers compared to *exo*-isomers, particularly in norbornenes with bulky substituents.[18−20] Unfortunately, the bulky substituents needed for high-performing polynorbornene membranes face the largest difficulties in polymerization because of steric interferences between the *endo*-monomer and metallocyclo- transition states during polymerization.[20,21] Difficulties arising from *endo*-monomer content are further compounded in the Diels−Alder route conventionally used for norbornene monomer synthesis. This route typically favors *endo*-isomer formation

Received: July 30, 2020
Accepted: August 26, 2020
Published: August 31, 2020

https://dx.doi.org/10.1021/acsmacrolett.0c00555
ACS Macro Lett. 2020, 9, 1363−1368

because of unfavorable steric effects in the *exo*-transition-state pathway and secondary orbital HOMO−LUMO interactions.[22]

In this study, we demonstrate the use of a reductive Mizoroki−Heck reaction recently applied to substituted norbornenes that yield solely *exo*-norbornene monomers for enhanced polymerizations.[23] Postulated mechanisms of this reaction show norbornadiene insertion with *exo*-face selectivity into aryl-Pd-halide intermediates, which later reductively eliminate to form solely *exo*-substituted norbornenes and tricyclononenes. We expect the increased side group stereoregularity to provide improvements in gas permeability[24] and also yield important consequences in fields that desire more uniform stereoregularity, especially the life sciences.

We show that the reductive Mizoroki−Heck reaction may be utilized to produce several *exo*-selective norbornene monomers with varying substituents. Examples of this include trimethylsilyl groups to confer backbone rigidity and improved gas transport properties[25] or propoxy groups to imbue alkoxy ether content promoting polymeric solubility. These monomers produced *exo*-selective ROMP and addition-type polynorbornenes at yields up to >99% and molecular weights up to 1.8 MDa. Furthermore, we demonstrate via XRD and DFT calculations that several of these polymers have regimes of frustrated chain-packing that enable solubility-controlled NGL separations. The addition-type tricyclononene polymer with trimethylsilyl substituents achieved higher C_4H_{10}/CH_4 selectivity performance compared to both addition-type alkoxysilyl polynorbornenes and commercially used rubbery PDMS membranes.

The reductive Mizoroki−Heck reaction produced monomers with pure *exo*-isomerism through several pathways, shown in Figure 1, by reacting aryl halides with norbornadiene. In one example, we synthesized the monomeric precursor bearing a trimethylsilyl group via the arylation of chlorotrimethylsilane.[26] The reductive Mizoroki−Heck reaction shown in pathway 2 used $[PdCl_2(PCy_3)_2]$ and $NaHCO_3$ to yield *exo*-norbornene monomer, whereas $[PdCl_2(PCy_3)_2]$ and Cs_2CO_3 in the absence of a reducing agent produced *exo* tricyclononene monomer in pathway 3. The key mechanistic differences between these two routes has been previously explored and are summarized in the SI.[23] Figure 2 shows the determination of monomeric *exo* purity using ^1H NMR spectroscopy, highlighting the olefinic regions of several norbornene monomers. The top spectrum shows a norbornene monomer produced via the Diels−Alder route yielding a mixture of *exo*- and predominately *endo*-monomers. Notably, the chemical shift difference between the olefinic protons is larger in the *endo*-isomer owing to their closer through-space proximity to the *endo*-substituent. The middle spectrum shows a norbornene monomer produced via the reductive Mizoroki−Heck reaction of pure *exo*-content, with smaller differences between olefinic protons shifts due to the *exo*-isomer pointing away from the double bond. The bottom spectrum of a tricyclononene monomer produced from the reductive Mizoroki−Heck route resolves into a single peak because of the "near" mirror plane of symmetry in the tricyclononene monomer.

Both norbornene and tricyclononene monomers were successfully polymerized via ROMP (Figure 1, pathways 4 and 5) and addition-type polymerizations (Figure 1, pathways 6 and 7) using previously described Grubbs first-generation catalyst and cationic Pd(II) systems, respectively.[14] Notably,

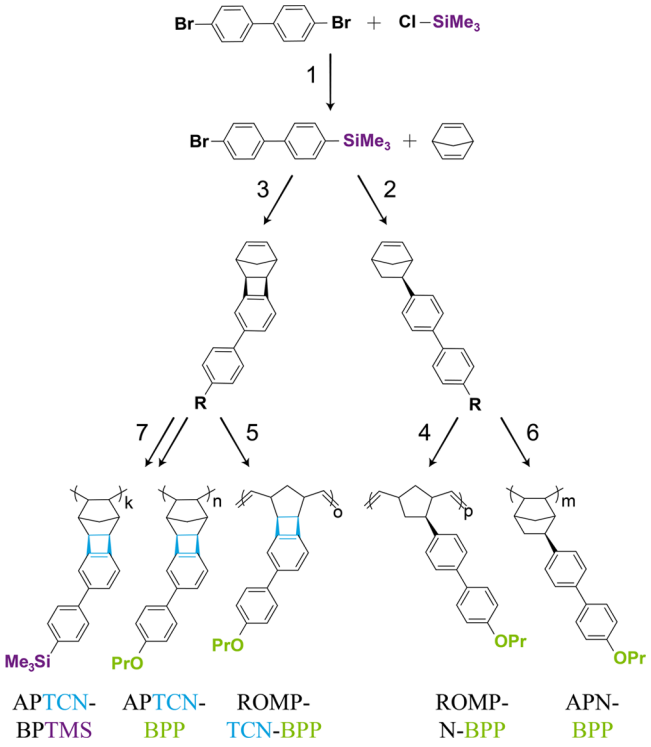

Figure 1. *Exo*-ROMP and addition-type polymers were synthesized from Grubbs first generation catalyst and cationic Pd(II) systems, respectively, using monomers derived from an *exo*-selective reductive Mizoroki−Heck reaction.

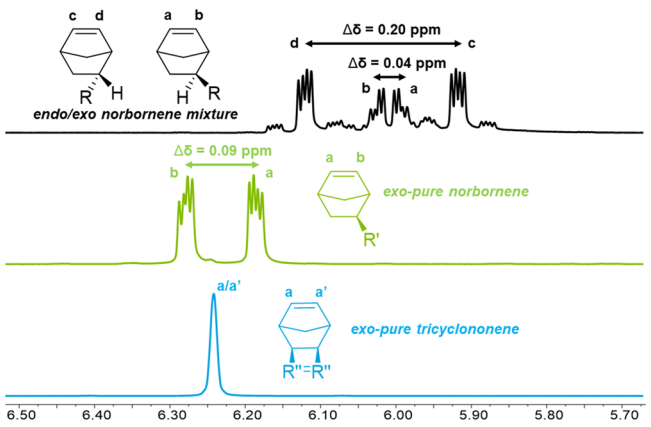

Figure 2. ^1H NMR spectra show larger chemical shifts for *endo*-isomers compared to *exo*-isomers.[20] In the top spectrum, R = $Si(OEt)_3$ in a Diels−Alder route derived norbornene.[14] In the middle and bottom spectra, R = substituted biphenyl moieties from the reductive Mizoroki−Heck reaction, resulting in *exo*-pure monomers.

both ROMP and addition-type polymers proceeded to high yields, whereas prior studies show lower yields in addition-type polymerizations with bulky substituents, especially compared to ROMP.[14,17,18,27] The higher yield of APTCN-BPP (>99%) compared to ROMP-TCN-BPP (94%) and identical APN-BPP and ROMP-N-BPP yields (88%) suggest that the polymerization yield in this class of polynorbornenes was controlled by monomer purity instead of polymerization mechanism. APTCN-BPTMS did exhibit less conversion (67%), but the demonstrated yield improvements in similar polymerizations (APN-BPP 44−88%) suggest enhanced yields are possible. The high yields demonstrated here add to the growing body of

https://dx.doi.org/10.1021/acsmacrolett.0c00555
ACS Macro Lett. 2020, 9, 1363−1368

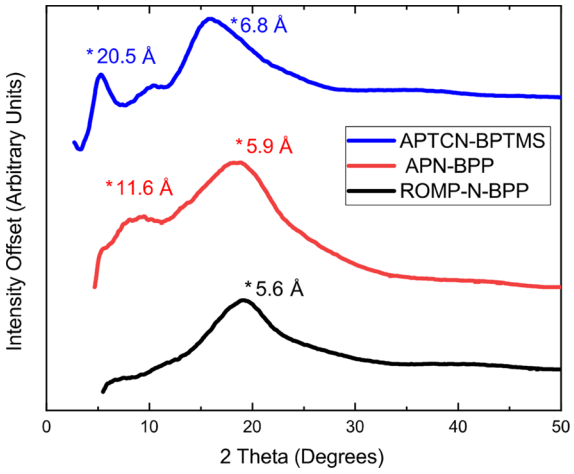

Figure 3. XRD traces show increased interchain spacing from ROMP to addition-type polynorbornenes to addition-type polytricyclononenes with trimethylsilyl substitution. Interchain *d*-spacing (d_{IC}) is denoted above the traces[30]

evidence that identifies *endo*-norbornene isomers as lowering yields in addition-type polymerizations.[20] The yields also demonstrate that the reductive Mizoroki−Heck reaction can produce *exo*-selective norbornene/tricyclononene monomers that successfully circumvent this challenge.

The reductive Mizoroki−Heck-derived polymers also showed increased molecular weights compared to addition-type polynorbornenes accessed through *endo*−*exo*-norbornene mixtures. Prior work using isomeric mixtures found that M_w ranged between 10 and 661 kDa, though differences in monomer structure, monomer/initiator ratio, and polymerization conditions preclude a direct comparison to the present work.[14,17−20,28] Similar to polymeric yield, reduced molecular weights have largely been attributed to steric difficulties endemic to the *endo*-norbornene isomer. In this study, addition-type polymers APTCN-BPP polymerized to M_w = 1780 kDa and APN-BPP polymerized to M_w = 720 kDa, both substantially higher than their respective ROMP polymers of 352 and 245 kDa. To the author's knowledge, these molecular weights are the highest reported for addition-type polynorbornenes and tricyclononene-based polymers, which is especially notable considering the large substituents utilized in this study.

Beyond increased yields and molecular weights, the *exo*-pure monomers also produced polymers of increased side group stereoregularity by simply excluding configurations derived from *endo*-monomers. Polynorbornenes produced in addition-type pathways typically contain highly complex configurations arising from *endo*- and *exo*-diastereomers and *R*,*S*-configurations, even assuming uniform *cis*-olefin addition.[29] The removal of *endo*-isomers eliminated four of six possible tetrads, leaving two *exo*-polymeric configurations produced from *R*- and *S*-enantiomers.

We utilized WAXD to study differences in interchain spacing between polymerization pathway (ROMP vs addition-type) and norbornene substituents. Figure 3 shows three diffractograms of norbornene polymers with maxima in interchain spacing (Å) denoted above the intensity plots. The bottom plot of ROMP-N-BPP is typical of many amorphous polymers developed for gas separations with interchain spacing maxima of 5.6 Å. The middle plot, for addition-type polynorbornene (APN-BPP), also has an additional region, indicating a second contribution of increased interchain spacing (11.6 Å), which we previously identified as evidence of polynorbornenes with a greater propensity for NGL separations.[14] Large interchain spacing favorably reduces diffusivity selectivity in this separation, which increases the dependence of solubility-controlled selectivity and allows for solubility-controlled permeation (e.g., C_3H_8/CH_4 > 1). The top diffractogram shows an addition-type tricyclononene polymer with biphenyl trimethylsilyl substituents featuring the highest interchain spacing (20.5 Å) of all polymers studied. We hypothesized that this polymer would be the most favorable for solubility-selective separations.

The pure gas permeabilities (Table 1) confirm the hypotheses based on XRD characterization that increased interchain spacing promoted enhanced gas permeability. Regarding polymeric backbone, permeabilities increase substantially from ROMP, to addition-type, and to tricyclononene motifs. Between pendant groups, the trimethylsilyl substituent shows an order of magnitude increase in permeability compared to biphenyl propoxy substitution in the tricyclononene derivative. For diffusion-controlled separations (e.g., CO_2/CH_4, He/N_2), increases in permeability lead to an expected concomitant decrease in selectivity. Notably, tricyclononene-based polymers demonstrated solubility-controlled permeation (C_3H_8/CH_4 and C_4H_{10}/CH_4 > 1) through their enhanced gas permeabilities compared to ROMP and APN polymers.

Mixed gas permeation at 500 and 800 psi, Table 2, shows greatly improved gas permeabilities and C_3H_8/CH_4 selectivities compared to the pure gas results. Under these conditions, all addition-type and tricyclononene-based polymers demon-

Table 1. Ideal Permeability of the Polymers

	P (Barrer)								
polymer	N_2	O_2	He	CH_4	CO_2	C_3H_8	C_4H_{10}	He/N_2	C_4H_{10}/CH_4
ROMP-N-BPP	0.46 (±0.02)	1.57 (±0.05)	6.94 (±0.39)	0.63 (±0.02)	8.33 (±0.07)			15.21 (±0.30)	
ROMP-TCN-BPP	0.67 (±0.15)	2.24 (±0.07)	9.49 (±0.49)	0.85 (±0.00)	12.52 (±1.51)			15.06 (±4.13)	
APN-BPP	1.17 (±0.18)	3.90 (±0.22)	11.85 (±0.70)	2.17 (±0.06)	27.46 (±1.43)			10.29 (±0.94)	
APTCN-BPP	3.39 (±0.02)	11.08 (±0.35)	25.76 (±0.58)	6.35 (±0.09)	76.97 (±3.55)	6.64 (±0.02)	178.99 (±12.19)	7.60 (±0.13)	28.20 (±2.31)
APTCN-BPTMS	40.86 (±5.41)	124.59 (±10.27)	152.36 (±10.30)	84.48 (±3.95)	713.91 (±46.05)	143.69 (±98.44)	1803.25 (±250.27)	3.77 (±0.37)	21.44 (±3.45)

https://dx.doi.org/10.1021/acsmacrolett.0c00555
ACS Macro Lett. 2020, 9, 1363−1368

Table 2. Mixed Gas Permeabilities and Selectivities of Polymers

		P (Barrer)						
polymer	*p* (psi)	CH_4	CO_2	C_2H_6	C_3H_8	C_4H_{10}	C_3H_8/CH_4	C_4H_{10}/CH_4
APN-BPP	500	23.96	143.97	64.17	84.30	189.23	3.52	7.89
		(±0.30)	(±0.92)	(±1.60)	(±3.48)	(±13.69)	(±0.10)	(±0.47)
	800	32.74	193.84	93.30	134.38	321.56	4.10	9.82
		(±0.36)	(±4.98)	(±0.63)	(±0.69)	(±0.66)	(±0.02)	(±0.13)
APTCN-BPP	500	46.39	252.55	138.60	208.09	506.36	4.48	10.89
		(±1.40)	(±6.47)	(±6.70)	(±15.68)	(±56.06)	(±0.20)	(±0.88)
	800	57.56	314.07	183.76	293.30	739.03	5.08	12.80
		(±3.23)	(±18.71)	(±14.19)	(±29.32)	(±82.01)	(±0.22)	(±0.71)
APTCN-BPTMS	500	279.60	1194.78	980.99	1827.76	4977.43	6.53	17.76
		(±59.76)	(±252.41)	(±214.11)	(±405.01)	(±1118.34)	(±0.05)	(±0.20)
	800	330.60	1430.95	1203.09	2340.46	6523.22	7.06	19.63
		(±68.00)	(±293.58)	(±259.97)	(±517.20)	(±1497.69)	(±0.11)	(±0.49)
APN-$Si(OEt)_3$	800	985.21			7765.77	18254.18	7.88	18.53
PDMS	800	1097.13			7890.85	15468.08	7.12	13.94

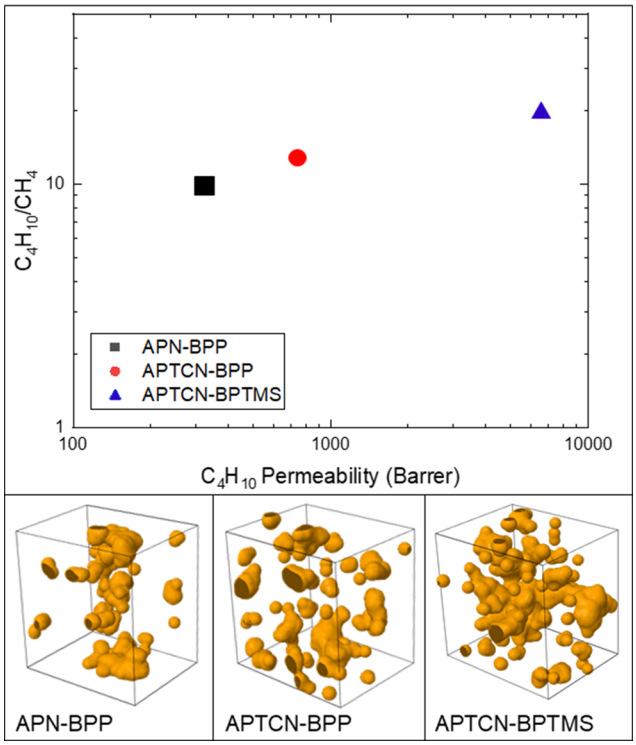

Figure 4. (upper) Permeation performance plot with simultaneous improvements in heavy hydrocarbon selectivity and permeability. (lower) Modeled free volume available for butane permeation. The cavity isosurface plots use a probe radius equal to 2.15 Å, half the kinetic diameter of butane.[36]

strate high performance in solubility-selective permeation. APTCN-BPTMS has the highest mixed gas selectivities of C_3H_8/CH_4 = 7.06 and C_4H_{10}/CH_4 = 19.63, which compares favorably to previously investigated alkoxysilyl addition-type polynorbornenes (APN-$Si(OEt)_3$) and commercialized state-of-the-art PDMS.[31] The improvement of mixed gas permeability and C_3H_8/CH_4 selectivity may be caused by the plasticizing five-component feed that actively swells the polymer with highly condensable propane and butane gas.[31] Pure gas measurements with propane at atmospheric pressure insufficiently plasticized the polymers tested, which resulted in relatively densified polymeric states. We hypothesize that plasticized states with enhanced free volume favorably promote enhanced sorption and permeability of hydrocarbon gases and beneficially reduces diffusivity-selectivity. Membrane testing with pressure increased from 500 to 800 psi confirms this phenomenon showing a simultaneous increase in heavy hydrocarbon permeabilities and mixed gas selectivities.

Mixed gas testing indicates polynorbornenes overcoming trade-off relationships between permeability and selectivity typically observed in membrane separations. This phenomenon is best observed within the mixed-gas transport performance (Figure 4, upper plot) of the top performing materials at 800 psi. The polymers with highest WAXD interchain spacing result in the highest hydrocarbon permeabilities and the hypothesized decrease in diffusivity selectivity results in improved solubility-driven C_4H_{10}/CH_4 selectivities. Figure 4 demonstrates that polymers may be rationally designed to have transport performance enhancements in both heavy hydrocarbon permeability and selectivity. We achieve this through varying the ring-strain from addition-type norbornenes to tricyclononenes and by incorporating bulky $SiMe_3$ side chain moieties compared to biphenyl propoxy groups. Our polymers incorporate the aforementioned design elements to enhance intrinsic free volume (rigid, contorted ring-strain, and poorly packing $-SiMe_3$ groups).

To better understand these effects at the molecular level, we constructed computational models of APN-BPP, APTCN-BPP, and APTCN-BPTMS. Oligomers of 20 repeat units were constructed in *cis*-disyndiotactic form, the preferred tacticity from catalytic insertion compared to random linkages between monomers.[13,25] Eight copies of the 20-mer were randomly inserted into a dilute box followed by simulated annealing using LAMMPS molecular modeling software[32] and the 21-step equilibration scheme developed by the Colina group.[33] Porosities of our equilibrated models were quantified with PoreBlazer code,[34] resulting in average system densities of 0.830, 0.860, and 0.898 and average fractional free volumes (FFV) of 0.339, 0.314, and 0.264, respectively, for APTCN-BPTMS, APTCN-BPP, and APN-BPP. The simulated FFV of 0.339 for APTCN-BPTMS (all *exo* side group content) was notably higher compared to an all *endo*-variant of APTCN-BPTMS computed in the SI (FFV = 0.277). Void spaces of our models were visualized with Jmol software,[35] where the effects of the contorted monomers and $SiMe_3$ groups are clearly visualized to provide greater FFV (Figure 4, bottom plot).

https://dx.doi.org/10.1021/acsmacrolett.0c00555
ACS Macro Lett. 2020, 9, 1363−1368

These models grant additional evidence that trimethylsilyl substituents improve FFV and chain spacing compared to biphenyl propoxy substituents, and that tricyclononene polymeric backbones have similar improvements compared to addition-type polymers. The FFV improvements translate to larger available void spaces for heavy hydrocarbon permeation and improved properties in reverse-selective membranes.

In summary, we introduce a novel route toward the production of *exo* ROMP and addition-type polynorbornenes and polytricyclononenes through the stereochemical control afforded by the reductive Mizoroki–Heck reaction. *Exo*-selective norbornenes offer several advantages compared to prior routes, including yields up to >99%, the highest molecular weights reported among addition-type polynorbornenes, and improved side group stereoregularity in polymeric microstructure. Addition-type polynorbornenes and polytricyclononenes demonstrate the increased polymeric chain-spacing necessary for solubility-selective membranes, confirmed by pure and mixed-gas permeation studies that show improved C_4H_{10}/CH_4 mixed gas selectivities compared to our first generation polynorbornenes and commercial PDMS. Computational modeling validates the effects of individual design elements that promoted increased FFV and gas separation performance for the design of next-generation materials. Future efforts may target large libraries of commercially available aryl halides that can imbue further chain rigidity and packing interruptions. We also anticipate that extending this work to other living-type norbornene polymerizations will unlock monodisperse polynorbornenes with greatly improved stereoregularity.

■ ASSOCIATED CONTENT

Supporting Information

The Supporting Information is available free of charge at https://pubs.acs.org/doi/10.1021/acsmacrolett.0c00555.

Detailed synthetic methods and full characterization of these materials (NMR, FTIR, TGA, GPC, XRD, and EA) (PDF)

■ AUTHOR INFORMATION

Corresponding Authors

Benjamin J. Sundell − *Aramco Research Center − Boston, Aramco Services Company, Boston, Massachusetts 02139, United States;* orcid.org/0000-0002-8041-2376; Email: benjamin.sundell@aramcoservices.com

John A. Lawrence, III − *Aramco Research Center − Boston, Aramco Services Company, Boston, Massachusetts 02139, United States;* orcid.org/0000-0001-8159-0636; Email: trey@c2sense.com

Authors

Daniel J. Harrigan − *Aramco Research Center − Boston, Aramco Services Company, Boston, Massachusetts 02139, United States;* orcid.org/0000-0002-5541-3481

Sibo Lin − *Aramco Research Center − Boston, Aramco Services Company, Boston, Massachusetts 02139, United States*

Tatiana P. Headrick − *Aramco Research Center − Boston, Aramco Services Company, Boston, Massachusetts 02139, United States*

Jeremy T. O'Brien − *Aramco Research Center − Boston, Aramco Services Company, Boston, Massachusetts 02139, United States*

William F. Penniman − *Aramco Research Center − Boston, Aramco Services Company, Boston, Massachusetts 02139, United States*

Nathan Sandler − *Aramco Research Center − Boston, Aramco Services Company, Boston, Massachusetts 02139, United States*

Complete contact information is available at: https://pubs.acs.org/10.1021/acsmacrolett.0c00555

Author Contributions

‡These authors contributed equally to this work. The manuscript was written through contributions of all authors. All authors have given approval to the final version of the manuscript.

Notes

The authors declare no competing financial interest.

■ ACKNOWLEDGMENTS

The authors thank Dr. Michele L. Ostraat for her helpful comments during manuscript preparation.

■ REFERENCES

(1) Elimelech, M.; Phillip, W. A. The future of seawater desalination: energy, technology, and the environment. *Science* **2011**, *333*, 712.

(2) Park, H. B.; Kamcev, J.; Robeson, L. M.; Elimelech, M.; Freeman, B. D. Maximizing the right stuff: The trade-off between membrane permeability and selectivity. *Science* **2017**, *356*, eaab0530.

(3) Sholl, D. S.; Lively, R. P. Seven chemical separations to change the world. *Nature* **2016**, *532*, 435.

(4) Merkel, T. C.; Zhou, M.; Baker, R. W. Carbon dioxide capture with membranes at an IGCC power plant. *J. Membr. Sci.* **2012**, *389*, 441.

(5) Galizia, M.; Chi, W. S.; Smith, Z. P.; Merkel, T. C.; Baker, R. W.; Freeman, B. D. 50th Anniversary Perspective: Polymers and Mixed Matrix Membranes for Gas and Vapor Separation: A Review and Prospective Opportunities. *Macromolecules* **2017**, *50*, 7809.

(6) Baker, R. W.; Low, B. T. Gas Separation Membrane Materials: A Perspective. *Macromolecules* **2014**, *47*, 6999.

(7) Lau, C. H.; Li, P.; Li, F.; Chung, T.-S.; Paul, D. R. Reverse-selective polymeric membranes for gas separations. *Prog. Polym. Sci.* **2013**, *38*, 740.

(8) Lin, H.; Van Wagner, E.; Freeman, B. D.; Toy, L. G.; Gupta, R. P. Plasticization-Enhanced Hydrogen Purification Using Polymeric Membranes. *Science* **2006**, *311*, 639.

(9) Yampolskii, Y.; Starannikova, L.; Belov, N.; Bermeshev, M.; Gringolts, M.; Finkelshtein, E. Solubility controlled permeation of hydrocarbons: New membrane materials and results. *J. Membr. Sci.* **2014**, *453*, 532.

(10) Grinevich, Y.; Starannikova, L.; Yampolskii, Y.; Gringolts, M.; Finkelshtein, E. Solubility controlled permeation of hydrocarbons in novel highly permeable polymers. *J. Membr. Sci.* **2011**, *378*, 250.

(11) Du, N.; Song, J.; Robertson, G. P.; Pinnau, I.; Guiver, M. D. Linear High Molecular Weight Ladder Polymer via Fast Polycondensation of 5,5′,6,6′-Tetrahydroxy-3,3,3′,3′-tetramethylspirobisindane with 1,4-Dicyanotetrafluorobenzene. *Macromol. Rapid Commun.* **2008**, *29*, 783.

(12) Tetsuka, H.; Isobe, K.; Hagiwara, M. Synthesis and Properties of Addition-Type Poly(norbornene)s with Siloxane Substituents. *Polym. J.* **2009**, *41*, 643.

(13) Potier, J.; Commarieu, B.; Soldera, A.; Claverie, J. P. Thermodynamic Control in the Catalytic Insertion Polymerization of Norbornenes as Rationale for the Lack of Reactivity of Endo-Substituted Norbornenes. *ACS Catal.* **2018**, *8*, 6047.

(14) Sundell, B. J.; Lawrence III, J. A.; Harrigan, D. J.; Vaughn, J. T.; Pilyugina, T. S.; Smith, D. R. Alkoxysilyl functionalized polynorbornenes with enhanced selectivity for heavy hydrocarbon separations. *RSC Adv.* **2016**, *6*, 51619.

(15) Lipian, J.; Mimna, R. A.; Fondran, J. C.; Yandulov, D.; Shick, R. A.; Goodall, B. L.; Rhodes, L. F.; Huffman, J. C. Addition Polymerization of Norbornene-Type Monomers. High Activity Cationic Allyl Palladium Catalysts. *Macromolecules* **2002**, *35*, 8969.
(16) Finkelshtein, E. S.; Makovetskii, K. L.; Gringolts, M. L.; Rogan, Y. V.; Golenko, T. G.; Starannikova, L. E.; Yampolskii, Y. P.; Shantarovich, V. P.; Suzuki, T. Addition-Type Polynorbornenes with Si(CH3)3 Side Groups: Synthesis, Gas Permeability, and Free Volume. *Macromolecules* **2006**, *39*, 7022.
(17) Gmernicki, K. R.; Hong, E.; Maroon, C. R.; Mahurin, S. M.; Sokolov, A. P.; Saito, T.; Long, B. K. Accessing Siloxane Functionalized Polynorbornenes via Vinyl-Addition Polymerization for CO2 Separation Membranes. *ACS Macro Lett.* **2016**, *5*, 879.
(18) Kim, D.-G.; Bell, A.; Register, R. A. Living Vinyl Addition Polymerization of Substituted Norbornenes by a t-Bu3P-Ligated Methylpalladium Complex. *ACS Macro Lett.* **2015**, *4*, 327.
(19) Kim, D.-G.; Takigawa, T.; Kashino, T.; Burtovyy, O.; Bell, A.; Register, R. A. Hydroxyhexafluoroisopropylnorbornene Block and Random Copolymers via Vinyl Addition Polymerization and Their Application as Biobutanol Pervaporation Membranes. *Chem. Mater.* **2015**, *27*, 6791.
(20) Tsai, S. D.; Register, R. A. Endo/Exo Reactivity Ratios in Living Vinyl Addition Polymerization of Substituted Norbornenes. *Macromol. Chem. Phys.* **2018**, *219*, 1800059.
(21) Freeman, B. D. Basis of Permeability/Selectivity Tradeoff Relations in Polymeric Gas Separation Membranes. *Macromolecules* **1999**, *32*, 375.
(22) Fernández, I.; Bickelhaupt, F. M. Origin of the "endo rule" in Diels-Alder reactions. *J. Comput. Chem.* **2014**, *35*, 371.
(23) Aida, F.; Sone, H.; Ogawa, R.; Hamaoka, T.; Shimizu, I. Palladium-catalyzed 5-exo-Selective Reductive Mizoroki-Heck Reaction of Aryl Chlorides with 2,5-Norbornadiene. *Chem. Lett.* **2015**, *44*, 715.
(24) Alentiev, D. A.; Bermeshev, M. V.; Starannikova, L. E.; Bermesheva, E. V.; Shantarovich, V. P.; Bekeshev, V. G.; Yampolskii, Y. P.; Finkelshtein, E. S. Stereoselective synthesis and polymerization of Exo-5-trimethylsilylnorbornene. *J. Polym. Sci., Part A: Polym. Chem.* **2018**, *56*, 1234.
(25) Mazo, M.; Balabaev, N.; Alentiev, A.; Yampolskii, Y. Molecular Dynamics Simulation of Nanostructure of High Free Volume Polymers with SiMe3 Side Groups. *Macromolecules* **2018**, *51*, 1398.
(26) Hanss, D.; Wenger, O. S. Conformational Effects on Long-Range Electron Transfer: Comparison of Oligo-p-phenylene and Oligo-p-xylene Bridges. *Eur. J. Inorg. Chem.* **2009**, *25*, 3778.
(27) Tetsuka, H.; Hagiwara, M.; Kaita, S. Addition-type poly(norbornene)s with siloxane substituents: synthesis, properties and nanoporous membrane. *Polym. J.* **2011**, *43*, 97.
(28) Maroon, C. R.; Townsend, J.; Gmernicki, K. R.; Harrigan, D. J.; Sundell, B. J.; Lawrence, J. A.; Mahurin, S. M.; Vogiatzis, K. D.; Long, B. K. Elimination of CO2/N2 Langmuir Sorption and Promotion of "N2-Phobicity" within High-Tg Glassy Membranes. *Macromolecules* **2019**, *52*, 1589.
(29) Janiak, C.; Lassahn, P. G. The Vinyl Homopolymerization of Norbornene. *Macromol. Rapid Commun.* **2001**, *22*, 479.
(30) Klug, H. D.; Alexande, L. E. *X-ray diffraction procedures for polycrystalline and amorphous materials*; Wiley: New York, 1964.
(31) Vaughn, J. T.; Harrigan, D. J.; Sundell, B. J.; Lawrence III, J. A.; Yang, J. Reverse selective glassy polymers for C3+ hydrocarbon recovery from natural gas. *J. Membr. Sci.* **2017**, *522*, 68.
(32) Plimpton, S. Fast Parallel Algorithms for Short-Range Molecular Dynamics. *J. Comput. Phys.* **1995**, *117*, 1.
(33) Abbott, L.; Hart, K. E.; Colina, C. *Polymatic*: a generalized simulated polymerizaton algorithm for amorphous polymers. *Theor. Chem. Acc.* **2013**, *132*, 1334.
(34) Sarkisov, L.; Harrison, A. Computational structure characterisation tools in application to ordered and disordered porous materials. *Mol. Simul.* **2011**, *37*, 1248.
(35) Jmol: an open-source Java viewer for chemical structures in 3D. http://www.jmol.org/.
(36) McKeen, L. W. In *Permeability Properties of Plastics and Elastomers*, 3rd ed.; McKeen, L. W., Ed.; William Andrew Publishing: Oxford, 2012; p 1.

https://dx.doi.org/10.1021/acsmacrolett.0c00555
ACS Macro Lett. 2020, 9, 1363−1368